



HAL
open science

Non viscous sensitivity analysis of noise generation mechanism in a low Mach number jet

Christophe Airiau, Tobias Ansaldi

► **To cite this version:**

Christophe Airiau, Tobias Ansaldi. Non viscous sensitivity analysis of noise generation mechanism in a low Mach number jet. 50th 3AF International Conference on Applied Aerodynamics, Mar 2015, Toulouse, France. hal-01695136

HAL Id: hal-01695136

<https://hal.science/hal-01695136v1>

Submitted on 29 Jan 2018

HAL is a multi-disciplinary open access archive for the deposit and dissemination of scientific research documents, whether they are published or not. The documents may come from teaching and research institutions in France or abroad, or from public or private research centers.



L'archive ouverte pluridisciplinaire **HAL**, est destinée au dépôt et à la diffusion de documents scientifiques de niveau recherche, publiés ou non, émanant des établissements d'enseignement et de recherche français ou étrangers, des laboratoires publics ou privés.



Open Archive TOULOUSE Archive Ouverte (OATAO)

OATAO is an open access repository that collects the work of Toulouse researchers and makes it freely available over the web where possible.

This is an author-deposited version published in : <http://oatao.univ-toulouse.fr/>
Eprints ID : 18320

To cite this version : Airiau, Christophe  and Ansaldi, Tobias 
Non viscous sensitivity analysis of noise generation mechanism in a low Mach number jet. (2015) In: 50th 3AF International Conference on Applied Aerodynamics, 29 March 2015 - 1 April 2015 (Toulouse, France). (Unpublished)

Any correspondence concerning this service should be sent to the repository administrator: staff-oatao@listes-diff.inp-toulouse.fr

NON VISCOUS SENSITIVITY ANALYSIS OF NOISE GENERATION MECHANISM IN A LOW MACH NUMBER JET

C. Airiau¹ and T. Ansal di²

¹ *IMFT, UMR 5502 CNRS/INP-UPS, Université de Toulouse, Allée du Pr. Camille Soula, 31400, Toulouse, France,
christophe.airiau@imft.fr*

² *IMFT, UMR 5502 CNRS/INP-UPS, Université de Toulouse, Allée du Pr. Camille Soula, 31400, Toulouse, France,
tobias.ansaldi@imft.fr*

The first step of the sensitivity analysis of some quadratic quantity related to acoustic waves with respect to any flow or wall disturbance is proposed in the configuration of subsonic jet flow. The generation of noise has been demonstrated to originate from convective instabilities that amplify in the jet stream. Several authors have investigated them through the Parabolized Stability Equations approach (PSE). The present work aims to develop the adjoint of the PSE to extract from a mathematically well posed problem the sensitivity coefficients which can be understood as gradient. The final objective is to propose some path of possible actuations in order to decrease noise emission in some jet flows. To date some trend can be given. The shape and the location of the maximum of sensitivity are strongly related to the radial and streamwise variation of the base flow. In particular the maximum of sensitivity is located along the border of the potential cone and seems to be well correlated with the location of the sound generation mechanism. In addition the sensitivity to axial momentum forcing is higher than to a radial momentum forcing. Finally the sensitivity increases when the perturbation is near to the exit of the nozzle.

INTRODUCTION

In the past many investigators [1–7] have suggested based to theoretical and experimental results that flow instabilities should be the dominant noise-generation mechanism for jet flows especially at high Mach number. In the same manner, more recent works [8–10] have shown that instabilities can play an important role even for subsonic jet noise amplification. In addition, a low computational cost model of the shear-layer instability modes in the co-axial jet based on the Parabolized Stability

Equation (PSE) has been developed and correlations between CFD results have been tested successfully [2, 4, 5, 10].

In the present works, a sensitivity analysis is performed for a subsonic inviscid single stream jet. The main goal is to identify the regions of the flow more sensitive to external momentum forcing and mass or heat injection. Sensitivity is equivalent to a gradient of any functional or quadratic integral [11]. This functional called E in this paper is the physical energy associated to the perturbed velocity, temperature and pressure. Mathematically it can be written as

a quadratic function of the full disturbance vector of the flow field as:

$$E = \frac{1}{2} \int_{x_0}^{x_f} E_x(x) dx, \quad (1)$$

with

$$E_x(x) = \int_0^\infty \mathbf{q}'^t M \mathbf{q}' m_r dr$$

where $\mathbf{q}' = (u'_x, u'_r, u'_\theta, \rho', p')^t$ is the state vector of the flow perturbation where components are respectively velocity, density and pressure disturbance and $\Omega = [x_0, x_f] \times [0, \infty]$ is the physical domain. For the computational domain $r \in [0, r_{max}]$, r_{max} far enough from the axis. Assuming a quasi-3D flow the coordinate θ is not required in the integral domain. The exponent t refers to the transpose of a matrix or a vector. The velocity are written in the cylindrical system of coordinates. The diagonal positive matrix M and the metric m_r are the way to introduce various kind of 'energy' definition. They are set respectively to identity I and to the radius r in the following.

Sensitivity coefficients can be therefore explained as how the response of any variation in the output of a system expressed as a mathematical functional can be apportioned to different sources of variation in the input of the model. Such analysis is common in different fields of engineering and in the field of fluid dynamics since it is closely related to optimization problems and optimal control [12, 13]. In the last 45 years the physical problem of receptivity and sensitivity of boundary layers flows were investigated in different theoretical, experimental and computational manners. Airiau et al [14] have demonstrated that receptivity coefficients and the approach based on adjoint equations [13] can be associated to an optimization problem and therefore they were strongly closed to sensitivity coefficients. Later it was used to perform optimal control in the laminar boundary layer flow [12, 15]. The use of adjoint equations in flow instability dates back to the early 1990s [16, 17], but did not become widespread until the late 2000s [18, 19] and finally the [20] where the concepts of sensitivity analysis with adjoint are spell out in details. Sensitivity analysis based on the adjoint of compressible Navier-Stokes equations have been recently derived [11, 21] and applied to optimal control studies of the two dimensional shear layer in the aeroacoustic framework. Some other examples of sensitivity can be found in the mesh optimization and in the optimization of structures.

In the present work, the sensitivity of a quasi-3D jet flow is investigated on the based of adjoint of the Parabolized Stability Equations (APSE). Emphasis

is made on the methodology. Validation and application to a turbulent jet flow is currently in progress. In this paper, only results for an incompressible and inviscid unstable base-flow are presented and discussed. In the next months, the same methodology will be coupled to a LES solver where a mean flow will be determined first for single stream and later to dual stream flow. The main objective is to investigate flow sensitivities to any disturbances and to define some new noise control strategies. The different steps of the methodology are briefly described in the next two sections. Section III shows validation and results and a conclusion ended the paper.

I- PARABOLIZED STABILITY EQUATIONS (PSE)

The flow disturbances are considered as the state variables of the model and their evolutions are assumed to be well defined by solving the PSE equations.

The PSE were initially proposed by Herbert and Bertolotti in 1991 [22], and some other authors during the same period [23] to study the linear and non linear development of Tollmien-Schlichting waves in boundary layers. Comparing to the local stability theory (LST) where the Orr-Sommerfeld equation are solved through an eigenvalue problem, the main advantage of the PSE are to take into account of the small streamwise variations of the base flow and of the disturbances directly in the formulation. The eigenvalue problem no longer exists and the PSE is set of partial differential equations (PDE) almost parabolic in the streamwise direction. The second advantage is that because of solving PDE source terms and various boundary conditions can be introduced leading to perform quite easily flow control and weakly non linear stability studies.

PSE were extended later after 2000 for jet flow [24–26]. In this paper, only linear PSE are considered, therefore the first step is the compressible Linearized Euler equations for an axial-symmetric flow in cylindrical coordinates (x, r, θ, t) written as:

$$L_{LEE} \mathbf{q}' = \mathbf{0}, \quad (2)$$

with

$$L_{LEE} = B + A_3 \frac{\partial}{\partial t} + A_2 \frac{\partial}{\partial \theta} + A_1 \frac{\partial}{\partial x} + A_0 \frac{\partial}{\partial r}$$

where $\mathbf{q}' = (u'_x, u'_r, u'_\theta, \rho', p')^t$ has been ever defined. The lengths are non-dimensionalized by the diameter D_j , the velocity by the streamwise exit velocity u_j , the density by ρ_j , the pressure by $\rho_j u_j^2$, the

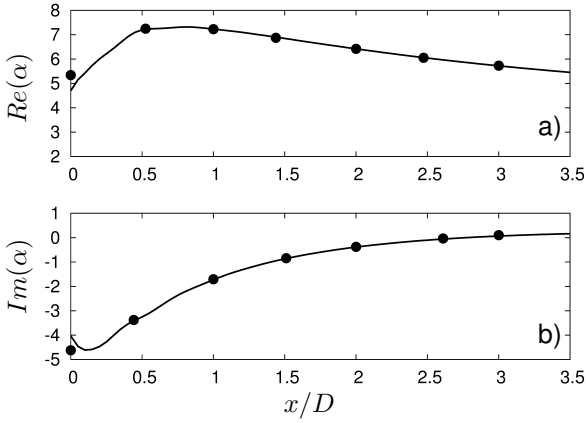


Figure 1: Comparison between present PSE and Yen et Messersmith PSE(o), 1998 streamwise wavenumber solution α . a) Real part of α , b) Imaginary part of α for a subsonic flow with $\omega = 1.2\pi$ and $m = 0$. See also [2].

time by D_j/u_j . The subscript "j" refers to the conditions at the jet exit.

The viscosity is neglected here because its role is quite negligible in the aeroacoustic studies of jet flow and in the sound generation and propagation. A_0, A_1, A_2, A_3 and B are matrices function of the base flow quantities.

Each line of the matrix L_{LEE} has been obtained from conservation equations:

$$L_{LEE}\mathbf{q}' = \begin{bmatrix} \text{continuity} \\ \text{momentum for } r \\ \text{momentum for } \theta \\ \text{momentum for } x \\ \text{energy} \end{bmatrix} = \mathbf{0} \quad (3)$$

An important assumption is made at this step. It is assumed that the axial evolution of large scale structures is not subject to nonlinear interactions, but is rather controlled by weakly non parallel mechanisms resulting from the divergence of the jet. The usual PSE assumption of small streamwise variations of the complex wave numbers is added inside the spatial theory framework, coming from the non local (also qualified as non-parallel) stability theory PSE developed by Herbert [22]. Finally the disturbance quantities can be written in the quasi normal mode form as:

$$\mathbf{q}' = \mathbf{q}(x, r) \chi(x) e^{i(m\theta - \omega t)} + c.c., \quad (4)$$

with

$$\chi(x) = \exp \left[i \int_{x_0}^x \alpha(\xi) d\xi \right]$$

In Eq. 4 \mathbf{q} is the shape function and it is assumed to be slowly varying in the x direction, $\alpha(x)$ is the

axial wavenumber, which is a complex function of the only streamwise variable, m is the fixed integer azimuthal wavenumber and the real number ω is the fixed angular frequency of the disturbance. x_0 is the inlet of the computational domain.

Substituting Eq. 4 into Eq. 2 we obtain the main part of the PSE equations. The question of keeping the term $\frac{\partial p}{\partial x}$ in the equation which let some ellipticity is not discussed there [22]. Finally a new set of PDE equations can be written:

$$L_{PSE}\mathbf{q} = \mathbf{0}, \quad (5)$$

with

$$L_{PSE} = i\alpha A_1 + i\omega A_3 + imA_2 + B + A_1 \frac{\partial}{\partial x} + A_0 \frac{\partial}{\partial r}$$

As usual in the stability problem the velocity disturbance is assumed to goes to zero when r goes to infinity.

By observing the decomposition of Eq. 4 it can be noticed that the streamwise change of the disturbance can be described by the product of the shape function and the exponential term. This ambiguity must be resolved by the introduction of an additional equation, called normalization or closure relationship, which imposes that the growth of the disturbance is absorbed by the wave function part of the decomposition $\chi(x)$, making sure that the shape function $\mathbf{q}(x, r)$ stays slowly varying in x . The streamwise dependence of the shape function is therefore distributed via the normalization. The definition of the normalization is based on the definition of the complex wave number respectively in the local and non local approach:

$$\begin{aligned} -i \frac{\partial \ln(q'_k)}{\partial x} &= \alpha, \quad \text{and} \\ -i \frac{\partial \ln(q'_k)}{\partial x} &= \alpha - i \frac{1}{q_k} \frac{\partial q_k}{\partial x} \end{aligned} \quad (6)$$

Naturally in the local stability theory the wave number is independent of radial direction r contrarily to the PSE theory case if the previous definition is kept. To remove this apparent dependency in r we imposing to $\alpha(x)$ the same definition as in the local stability and after few steps we found:

$$\int_0^\infty \bar{q}_k \frac{\partial q_k}{\partial x} m_r dr = 0, \quad (7)$$

or more generally:

$$\mathcal{N}(\mathbf{q}) = \int_0^\infty (N\bar{\mathbf{q}})^t \frac{\partial N\mathbf{q}}{\partial x} m_r dr = 0$$

The matrix N can let choose which components of the state vector are used in the closure relation. The choice of another specific normalization would not change the value of the physical disturbance, as soon as this normalization removes the waviness and growth of the disturbance from the shape function to include it in the exponential term as, explained by [4, 22, 23].

The system with the unknown (\mathbf{q}, α) is quasi-parabolic because an residual ellipticity due to the normalization condition and a streamwise pressure gradient term. It is solved numerically using a streamwise marching solution starting from the initial condition at $x = x_0$ which is set as the solution of the local approach(LST).

In the present work the PSE code called 'Paseq' has been designed, written and validated by the ONERA [2]. A comparison with the pioneer work of Yen et al. [5] is shown in Fig. 1, where the base flow is an analytical flow, for an incompressible jet:

II- SENSITIVITY WITH ADJOINT PSE

In the following the sensitivity equations are derived in the case of a small source forcing is applied as source term of the PSE as:

$$\chi L_{PSE} \mathbf{q} = \mathbf{f} \quad \text{and} \quad \int_0^\infty \bar{\mathbf{q}}^t \frac{\partial \mathbf{q}}{\partial x} r dr = 0 \quad (8)$$

As the initial state let us consider $\mathbf{f} = \mathbf{0}$ (no forcing). The sensitivity S_{f_k} is therefore the gradient of E with respect to any component of \mathbf{f} , f_k , translated mathematically as the relationship

$$\delta E(f_k) = \langle S_{f_k}, \delta f_k \rangle_\Omega \quad (9)$$

where the brackets $\langle u, v \rangle_\Omega$ indicates an integral inner product in the complex plane defined by over the computational domain Ω :

$$\langle u, v \rangle_\Omega = \int_\Omega \bar{v} u d\Omega = \int_{x_0}^{x_f} \int_0^\infty \bar{u} v r dr dx, \quad (10)$$

where overbar denotes complex conjugate. Formaly it can be written :

$$S_{f_k} = \nabla E_{f_k}(f_k = 0) = \left[\frac{\partial E}{\partial f_k} \right]_{f_k=0} \quad (11)$$

It is finally interpreted as how the variation in the output E can be apportioned to variation in the input δf_k around the unforced condition. In case of flow control problem or optimization problem, the forcing \mathbf{f} is naturally non zero.

To determine the sensitivity coefficients a Lagrangian functional is introduced, as it is currently done in optimal control or optimization problem. All arguments in this new functional are assumed independent of one another. We have:

$$\mathcal{L}(\mathbf{q}, \mathbf{f}, \alpha, \hat{\mathbf{q}}^*, \gamma) = E - \langle \hat{\mathbf{q}}^*, \chi L_{PSE} \mathbf{q} - \mathbf{f} \rangle_\Omega - \langle \gamma, \int_0^\infty \bar{\mathbf{q}}^t \frac{\partial \mathbf{q}}{\partial x} r dr \rangle_x + c.c. \quad (12)$$

In Eq. 12 we also consider the complex conjugate c.c. of the inner products to get real values. We have defined a new inner product $\langle \cdot, \cdot \rangle_x$ which is very similar to the first one but the integral is defined along the streamwise coordinate x . The vector $\hat{\mathbf{q}}^*$ and the complex number γ are some Lagrange multipliers associated to the full PSE systems including the normalization condition. Past work [13] has shown that $\hat{\mathbf{q}}^*$ is more conveniently written in a manner similar to the direct variables, i.e., by the introduction of a wave-like part:

$$\hat{\mathbf{q}}^*(x, y) = \mathbf{q}(x, y) \chi^*(x) \quad (13)$$

with

$$\chi^*(x) = i \exp \left[\int_{x_f}^{x_0} \bar{\alpha}(\xi) d\xi \right]$$

Taking into account Eq. 12 is an originality of this work and is necessary to get a mathematically well-posed problem.

Since the full PSE equations are equal to zero it is quite obvious that the variation of the Lagrangian functional is equal to the variation of the output quantity E : $\delta \mathcal{L} = \delta E$ and they have both the same gradient with respect to the state vector \mathbf{q} . Let us write formally the variation of the Lagrangian functional as :

$$\delta \mathcal{L} = \frac{\partial \mathcal{L}}{\partial \mathbf{q}} \delta \mathbf{q} + \frac{\partial \mathcal{L}}{\partial \mathbf{f}} \delta \mathbf{f} + \frac{\partial \mathcal{L}}{\partial \mathbf{q}^*} \delta \mathbf{q}^* + \frac{\partial \mathcal{L}}{\partial \alpha} \delta \alpha + \frac{\partial \mathcal{L}}{\partial \gamma} \delta \gamma \quad (14)$$

Eq. 14 has to be developed by introducing the PSE equations and calculate the variations of these equations with respect to the state vector $\mathbf{q}(x, r)$ and the complex wave number $\alpha(x)$.

Futhers details are given at the appendix.

The sensitivity coefficient S_{f_k} is found as the factor term of δf_k :

$$S_{f_k} = \nabla \mathcal{L}_{f_k} = \frac{\bar{\chi}(x_f)}{\bar{\chi}(x)} q_k^*(x, r) \quad (15)$$

where x_f is the end of the domain and q_k^* is the k component of the Lagrange multiplier vector \mathbf{q}^* . All

the other gradients with respect to each independent argument of the Lagrangian functional must be cancelled; this requirement is expressed by employing Fréchet differentiation in the (generic) direction δa , e.g.,

$$\frac{\partial \mathcal{L}}{\partial a} \delta a = \lim_{\varepsilon \rightarrow 0} \frac{\mathcal{L}(a + \varepsilon \delta a) - \mathcal{L}(a)}{\varepsilon} \quad (16)$$

Their derivations require a series of integration by parts to factorize the variations $\delta \mathbf{q}^*$, $\delta \mathbf{q}$, $\delta \gamma$, $\delta \alpha$ and $\delta \mathbf{f}$. The gradient with respect to the state vector lead to the so-called adjoint equations (APSE) where the adjoint state \mathbf{q}^* is solution of :

$$L_{APSE}^* \mathbf{q}^* = \mathbf{g}(\gamma, \mathbf{q}) \quad (17)$$

coupled with the new closing condition ($\frac{\partial \mathcal{L}}{\partial \alpha} \delta \alpha = 0$). This new closure relation can be reduced only to :

$$E_x + \chi(x_f) \frac{\partial}{\partial x} \langle \mathbf{q}^*, A_1 \mathbf{q} \rangle_r = 0 \quad (18)$$

with $\langle u, v \rangle_r = \int_0^\infty \bar{u} v r dr$.

The other part leads after some calculations and integration by part to obtain the boundary conditions of the adjoint state \mathbf{q}^* when $r \rightarrow \infty$ and to the so-called terminal condition of the adjoint problem. In fact, the adjoint equations are to be integrated upwinding from x_f to x_0 . The initial condition of the adjoint problem is therefore a 'terminal' condition.

The calculation are quite close to those found in [12] where the adjoint equation were obtained for an optimal control of the boundary layer instabilities. Determining the terminal condition is quite complex, since all the equations have to be detailed. In this particular case where the output E is defined in the whole computational domain, $\mathbf{q}^*(x_f, r) = 0$ is the "terminal" solution.

Introducing a wall forcing instead of a source forcing will not change the methodology, and results can be quickly found by adding some few developments in the previous equations as demonstrated in [15].

III- VALIDATION AND RESULTS

The subsonic base flow is determined from the analytical expression given firstly by Crow and Champagne [27] and found as well in [4] and [5].

The linear PSE results are given in Fig. 1.

The mean flow is given by:

$$\tilde{u}_x = \frac{1}{2} \left\{ 1 + \tanh \left[\frac{1}{8\Theta} \left(\frac{1}{2r} - 2r \right) \right] \right\} \quad (19a)$$

$$\Theta = 0.03x + 0.02 \quad (19b)$$

The non-dimensional mean pressure and density are assumed uniform in the solution domain and respectively equal to $\tilde{p} = \frac{1}{\gamma M^2}$ and $\tilde{\rho} = 1$. The mean radial velocity $\tilde{u}_r(x, r)$ is computed from the continuity equation. The computations were performed for Mach number $M_j = 0.01$ with the axisymmetric instability mode, $m = 0$ and a Strouhal number of 0.6.

The Physical domain of interest starts at the nozzle exit, $x = 0$.

A sixth order compact difference scheme [28] is used in the radial direction. The streamwise derivative, $\frac{\partial \mathbf{q}^*}{\partial x}$, is approximated by the backward finite-difference form $(\mathbf{q}_j^* - \mathbf{q}_{j-1}^*)/\Delta x$. The closure relation is solved with a Newton-Raphson algorithm and convergence is fast, less than 10 iterations with γ for each streamwise location x , the iteration is repeated until a relative error smaller than 10^{-5} . The state perturbation $\mathbf{q}(x)$ and the complex wave number α are required and have to be saved when running in the first step the PSE problem.

The APSE computations have been validated by following the steps outlined below:

- PSE code have been modified in order to solve:

$$\chi L_{PSE} \mathbf{q} = \mathbf{f}_k \quad (20)$$

where \mathbf{f}_k is the vector with f_k in the k-th position and zero otherwise.

- The variation of the quadratic function δE is computed as a difference between Eq. 20 and Eq. 5, after two PSE runs:

$$\delta E = E(\delta f_k) - E(0) \quad (21)$$

- The variation of the quadratic function δE is computed following APSE theory:

$$\delta E = \int_{\Omega} \frac{\bar{\chi}(x_f)}{\bar{\chi}} q_k^* \delta f_k d\Omega \quad (22)$$

Results of Eq. 22 shown a very favourably agreement compared to the direct approach Eq. 21 for forcing acting in continuity, and axial-momentum equations, as displayed in Fig. 3. Similar results have been found for forcing acting in Energy and r-momentum equations.

The small forcing δf_k is chosen as:

$$\delta f_k = \frac{\varepsilon}{|\delta f_k|^2} \exp(-\sigma_x(x - \tilde{x})^2 - \sigma_r(r - \tilde{r})^2) \quad (23)$$

Where (\tilde{x}, \tilde{r}) is the central location of the forcing and ε is the value of the integral volume of δf_k ,

x	r	σ_x	σ_r	ε
0.6	0.49	50	50	10^{-2}
0.7	0.48	30	30	10^{-2}
0.8	0.47	30	30	10^{-2}
0.9	0.46	30	30	10^{-2}
1.0	0.45	30	30	10^{-2}
1.1	0.44	30	30	10^{-2}
1.2	0.43	30	30	10^{-2}

Table 1: Values of the coefficient used for the validation at different spatial position

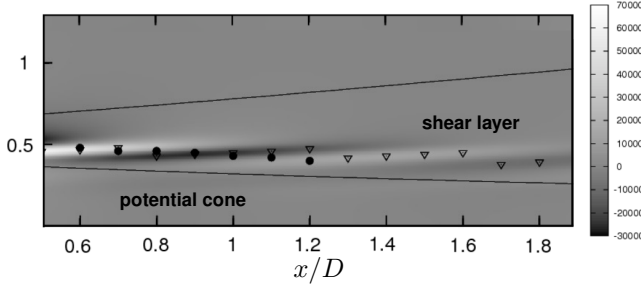


Figure 2: Isolines of spatial distribution of S_{f_4} , with ∇ are plotted the maximum of the sensitivity for different stream-wise positions, with \bullet are plotted the (\hat{x}, \hat{r}) used for validate de APSE.

$\int_{\Omega} \delta f_k d\Omega = \varepsilon$. This Gaussian function, Eq. 23 is set in the k-th line of the Eq. 3 and it acts in a restricted region of the domain (see Fig. 2). The values of the difference coefficients used to define f_k are shown in Tab. 1.

Forcing smaller and more localized in the position nearest from the exit of the nozzle is required in order to avoid modifications of the initial condition $q(0, r)$. The locations of the forcing have been chosen just out of the potential core where the sensitivity is high, see Fig. 2 and, because the arbitrary of the locations tested, they are simply placed along a straight line.

The variations of the total energy E with respect to forcing acting in the continuity, momentum and energy equation are shown in Fig. 4.

We can see that the shape and the location of the maximum of sensitivity are strongly related to the radial and streamwise variation of the base flow. In particular the maximum of sensitivity is located along the border of the potential cone and is well correlate with the location of the sound generation mechanism. A comparative study has to be done by defining some non dimensional gradient to compare the sensitivity coefficient of each PSE equations. However we can even conclude that sensitivity to axial

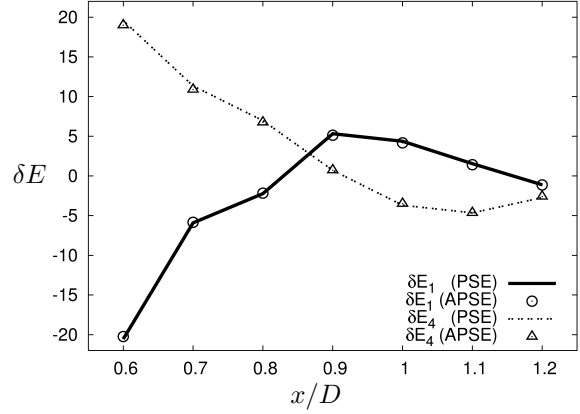


Figure 3: Comparison between results from Eq. 21 (lines) and Eq. 22 (symbols) is made.

momentum forcing is much higher than to a radial momentum forcing.

Another important point is that the sensitivity increases when the streamwise coordinate decreases. That makes sense since it is natural to reduce as soon as possible the mechanism of noise generation if the aim is to reduce noise emission.

IV- CONCLUSIONS

As conclusion a first sensitivity model of adjoint PSE equations has been derived in the case of jet flow instability. The goal will be to investigate some noise control strategy in a single and later in dual stream jet. First results concern a laminar flow, but we currently couple the analysis to a LES code in order to analyse stability and sensitivity from a base flow extract from a Large Eddy Simulations.

Another point will be in the near future to couple the stability solver to a far-field sound propagation approach and to propose the sensitivity of the full model. Many questions remains relative to the location and the quality of the coupling between the PSE pressure disturbance and the far-field zone as it have been discussed in [2, 7, 12, 24].

ACKNOWLEDGMENTS

This work has been supported by the European Community as part of the FP7-PEOPLE-2012-ITN AeroTraNet 2. We would like to thanks J.P. Brazier and O. Léon from ONERA Toulouse for having provided the PSE code 'Pasteq'. This work was performed using HPC resources from CALMIP (grant

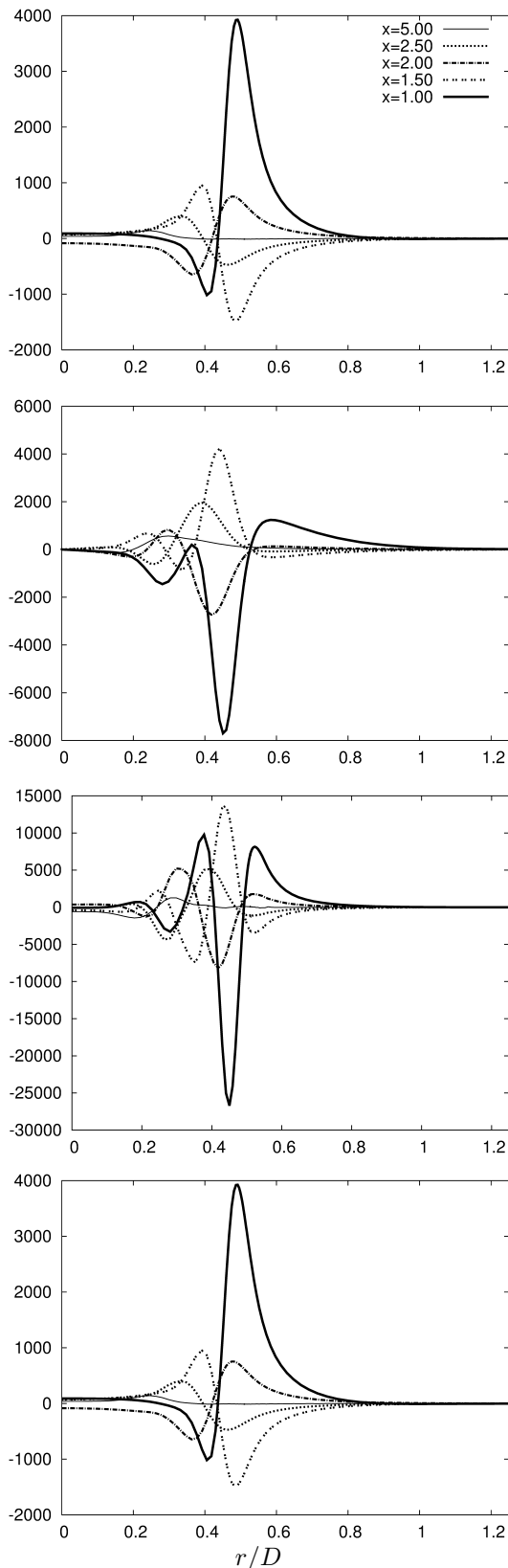


Figure 4: From top the bottom we have respectively, the gradient of E with respect to the forcing acting in the continuity, r -momentum, x -momentum and energy equation at different fixed position in the stream-wise direction ($x = 5.0, 2.5, 2.0, 1.5, 1.0$)

2014-24).

References

- [1] Tam, D. E., C. K. W. & Burton (1984) Sound generated by instability waves of supersonic flows. part 1.. two-dimensional mixing layers. *J. Fluid Mech.*, **138**, 249–271.
- [2] Léon, J.-P., O. & Brazier (2011) Application of linear Parabolized Stability Equations to a subsonic coaxial jet. *AIAA/CEAS, 32nd Aeroacoustics Conference*, no. AIAA 2011-2839.
- [3] Ray, P. K., Lawrence, C., Cheung, C., and Lele, S. K. (2009) On the growth and propagation of linear instability waves in compressible turbulent jets. *Phys. Fluids*, **21**.
- [4] Piot, E., Casalis, G., Muller, F., and Bailly, C. (2006) Investigation of the PSE approach for subsonic and supersonic hot jets. detailed comparison with les and linearized euler equations results. *aeroacoustic*, **5**, 361–393.
- [5] Yen, C. C. and Messersmith, N. L. (1998) Application of Parabolized Stability Equations to the prediction of jet instabilities. *AIAA/ASME, 36th Conference*, no. AIAA A98-16227.
- [6] Tam, C. K. W. (1971) Directional acoustic radiation from a supersonic jet generated by shear layer instability. *J. Fluid Mech.*, **46**, 757–768.
- [7] Suzuki, T. and Colonius, T. (2006) Instability waves in a subsonic round jet detected using a near-field phased microphone array. *J. Fluid Mech.*, **565**, 197–226.
- [8] Tam, C. K. W., Viswanathan, K., Ahuja, K. K., and Panda, J. (2008) The sources of jet noise: experimental evidence. *J. Fluid Mech.*, **615**, 253–292.
- [9] Reba, R., Narayanan, S., and Colonius, T. (2010) Wave-packet models for large-scale mixing noise. *Int. J. Aeroacoustics*, **9**, 533–558.
- [10] Ladeinde, F., Alabi, K., Colonius, T., Gudmundsson, K., Schlinker, R., and Reba, R. (2010) An integrated RANS-PSE-wave packet tool for the prediction of subsonic and supersonic jet noise. No. AIAA 2010-4021.
- [11] Pralits, J. O., Airiau, C., Hanifi, A., and Henningson, D. S. (2000) Sensitivity analysis using adjoint parabolized stability equations for

- compressible flows. *Flow Turbul. Combust.*, **65**, 321–346.
- [12] Walther, S., Airiau, C., and Bottaro, A. (2001) Optimal control of Tollmien-Schlichting waves in a developing boundary layer. *Phys. Fluids*, **13**, 2087–2096.
- [13] Airiau, C. (2000) Non-parallel acoustic receptivity of a Blasius boundary layer using an adjoint approach. *Flow Turbul. Combust.*, **65**, 347–367.
- [14] Airiau, C., Walther, S., and Bottaro, A. (2002) Boundary layer sensitivity and receptivity. *C.R. Mecanique*, **330**, 259–265.
- [15] Airiau, C., Bottaro, A., Walther, S., and Legendre, D. (2003) A methodology for optimal laminar flow control : Application to the damping of tollmien-schlichting waves in a boundary layer. *Phys. Fluids*, **15**, 1131–1145.
- [16] Hill, D. C. (1992) A theoretical approach for analyzing the re-stabilization of wakes. *NASA*.
- [17] Hill, D. C. (1995) Adjoint systems and their role in the receptivity problem for boundary layers. *J. Fluid Mech.*, **292**, 183:204.
- [18] Giannetti, F. and Luchini, P. (2007) Structural sensitivity of the first instability of cylinder wake. *J. Fluid Mech.*, **581**, 167:197.
- [19] Marquet, O., Sipp, D., and Jaquin, L. (2008) Sensitivity analysis and passive control of cylinder flow. *J. Fluid Mech.*, **615**, 221:252.
- [20] Luchini, P. and Bottaro, A. (2014) Adjoint equations in stability analysis. *Annu. Rev. Fluid Mech.*, **46**, 1–30.
- [21] Spagnoli, B. and Airiau, C. (2008) Adjoint analysis for noise control in a two-dimensional compressible mixing layer. *Computers and Fluids*, **37**, 475–486.
- [22] Herbert, T. (1997) Parabolized stability equations. *Annu. Rev. Fluid Mech.*, **29**, 245–283.
- [23] Airiau, C. and Casalis, G. (1993) Boundary layer linear stability using a system of parabolic equations. *Rech. Aérop.*, **5**, 57–68.
- [24] Cheung, L. C. and Lele, S. K. (2004) Acoustic radiation from subsonic and supersonic mixing layers with nonlinear PSE. No. AIAA 2004-0363.
- [25] Cheung, L. C., Bodony, D. J., and Lele, S. K. (2007) Noise radiation predictions from jet instability waves using a hybrid nonlinear PSE-acoustic analogy approach. No. AIAA 2007-3638.
- [26] Ray, P. K. and Lele, S. K. (2007) Sound generated by instability wave/shock-cell interaction in supersonic jets. *J. Fluid Mech.*, **587**, 173–215.
- [27] Crow, S. C. and Chamapagne, F. H. (1971) Orderly structure in jet turbulence. *J. Fluid Mech.*, **48**, 547–591.
- [28] Lele, S. K. (1992) Compact finite difference schemes with spectral-like resolution. *J. Comput. Phys.*, **103**, 16–42.

APPENDIX: PSE MATRICES

$$A_0 = \begin{bmatrix} 0 & \tilde{\rho} & 0 & \tilde{u}_r & 0 \\ 0 & \tilde{\rho}\tilde{u}_r & 0 & 0 & 1 \\ 0 & 0 & \tilde{\rho}\tilde{u}_r & 0 & 0 \\ \tilde{\rho}\tilde{u}_r & 0 & 0 & 0 & 0 \\ 0 & 0 & 0 & -\tilde{u}_r & \tilde{\rho}\tilde{u}_r M^2 \end{bmatrix}$$

$$A_1 = \begin{bmatrix} \tilde{\rho} & 0 & 0 & \tilde{u}_x & 0 \\ 0 & \tilde{\rho}\tilde{u}_x & 0 & 0 & 0 \\ 0 & 0 & \tilde{\rho}\tilde{u}_x & 0 & 0 \\ \tilde{\rho}\tilde{u}_x & 0 & 0 & 0 & 1 \\ 0 & 0 & 0 & -\tilde{u}_x & \tilde{\rho}\tilde{u}_x M^2 \end{bmatrix}$$

$$A_2 = \begin{bmatrix} 0 & 0 & \tilde{\rho} & 0 & 0 \\ 0 & 0 & 0 & 0 & 0 \\ 0 & 0 & 0 & 0 & 1 \\ 0 & 0 & 0 & 0 & 0 \\ 0 & 0 & 0 & 0 & 0 \end{bmatrix}$$

$$A_3 = \begin{bmatrix} 0 & 0 & 0 & 1 & 0 \\ 0 & \tilde{\rho} & 0 & 0 & 0 \\ 0 & 0 & \tilde{\rho} & 0 & 0 \\ \tilde{\rho} & 0 & 0 & 0 & 1 \\ 0 & 0 & 0 & -1 & \tilde{\rho}M^2 \end{bmatrix}$$

$$B = \begin{bmatrix} \frac{\partial \tilde{\rho}}{\partial x} & \tilde{\rho} + \frac{\partial \tilde{\rho}}{\partial r} & 0 & \frac{\tilde{u}_r}{r} + \frac{\partial \tilde{u}_x}{\partial x} \frac{\partial \tilde{u}_r}{\partial r} & 0 \\ \tilde{\rho} \frac{\partial \tilde{u}_r}{\partial x} & \tilde{\rho} \frac{\partial \tilde{u}_r}{\partial r} & 0 & 0 & 0 \\ 0 & 0 & \frac{\tilde{\rho}\tilde{u}_r}{r} & 0 & 0 \\ \tilde{\rho} \frac{\partial \tilde{u}_x}{\partial x} & \frac{\partial \tilde{\rho}}{\partial r} & 0 & 0 & 0 \\ -\frac{\partial \tilde{\rho}}{\partial x} & -\frac{\partial \tilde{\rho}}{\partial x} & 0 & 0 & 0 \end{bmatrix}$$

APPENDIX: APSE EQUATION

Procedure

Imposing all the different directional derivatives must vanish with exception of $\frac{\partial \mathcal{L}}{\partial \mathbf{f}} \delta \mathbf{f}$ we found:

$$\begin{aligned} \frac{\partial \mathcal{L}}{\partial \mathbf{q}} \delta \mathbf{q} &= \left\langle \chi_f \left(A^T + B^T - \frac{\partial A_1^H}{\partial x} - \frac{\partial A_0^T}{\partial r} - \frac{1}{r} A_0^T \right) \bar{\mathbf{q}}^*, \delta \mathbf{q} \right\rangle_{\Omega} \\ &- \left\langle \chi_f A_1^T \frac{\partial \bar{\mathbf{q}}^*}{\partial x} + \chi_f A_0^T \frac{\partial \bar{\mathbf{q}}^*}{\partial r}, \delta \mathbf{q} \right\rangle_{\Omega} \\ &+ \langle \chi_f A_{1f}^T \bar{\mathbf{q}}_f^*, \delta \mathbf{q}_f \rangle_r \\ &+ [\langle \chi_f A_0^T \bar{\mathbf{q}}^* r, \delta \mathbf{q} \rangle_x]_{r=0} \\ &+ [\langle \chi_f A_0^T \bar{\mathbf{q}}^* r, \delta \mathbf{q} \rangle_x]_{r=\infty} \\ &+ \left\langle \gamma \frac{\partial \bar{\mathbf{q}}}{\partial x} \delta \mathbf{q} - \frac{\partial (\tilde{\gamma} \bar{\mathbf{q}})}{\partial x} \delta \mathbf{q} \right\rangle_{\Omega} \\ &+ \langle \tilde{\gamma}_f \bar{\mathbf{q}}_f, \delta \mathbf{q}_f \rangle_r \\ &- \int_{x_0}^{x_f} \int_0^{\infty} 2\chi \bar{\chi} \bar{\mathbf{q}} \delta \mathbf{q} r dr + c.c. \end{aligned}$$

$$\begin{aligned} \frac{\partial \mathcal{L}}{\partial \alpha} \delta \alpha &= 2 \left\langle \left(\int_0^{\infty} \chi \bar{\chi} \bar{\mathbf{q}} r dr \right), \int_{x_0}^x \delta \alpha d\xi \right\rangle_x \\ &- \chi_f \left\langle \int_0^{\infty} \frac{\partial (\bar{\mathbf{q}}^* A_0 \mathbf{q})}{\partial x} r dr, \int_{x_0}^x \delta \alpha d\xi \right\rangle_x \\ &+ \chi_f \langle \bar{\mathbf{q}}_f^* A_{0f} \mathbf{q}_f, \delta \alpha_f \rangle_r c.c. \end{aligned}$$

with $A = i\alpha A_1 + imA_2 - i\omega A_3$, $\chi_f = \chi(x_f) = \bar{\chi}^*(x)\chi(x)$ and the subscript "f" beside a variable indicates its value at $x = x_f$.

Imposing:

$$\begin{aligned} \frac{\partial \mathcal{L}}{\partial \mathbf{q}^*} \delta \mathbf{q}^* &= 0 \\ \frac{\partial \mathcal{L}}{\partial \gamma} \delta \gamma &= 0 \end{aligned}$$

we obtain respectively Eq. 5 and Eq. 7.

Adjoint Parabolized Stability Equations

Since all variations are arbitrary, except at boundaries where the conditions are fixed (such as, for example, at $x = x_0$), the different integrals vanish if the following Euler-Lagrange equations are satisfied:

$$L_{PSE}^* \mathbf{q}^* = \mathbf{g}(\mathbf{q}, \gamma)$$

with

$$\begin{aligned} L_{PSE}^* &= -\frac{1}{r} A_0^H + A^H + B^H - \frac{\partial A_1^H}{\partial x} - \frac{\partial A_0^H}{\partial r} \\ &- A_1^H \frac{\partial}{\partial x} - A_0^H \frac{\partial}{\partial r} \end{aligned}$$

and

$$\mathbf{g}(\mathbf{q}, \gamma) = \frac{1}{\bar{\chi}_f} \left[(\gamma - \bar{\gamma}) \frac{\partial \mathbf{q}}{\partial x} + \left(\frac{\partial \gamma}{\partial x} + \chi \bar{\chi} \right) \mathbf{q} \right]$$

closing relation:

$$\int_0^{\infty} \left(i\chi \bar{\chi} \bar{\mathbf{q}} \mathbf{q} + \chi_f \frac{\partial (\bar{\mathbf{q}}^* A_0 \mathbf{q})}{\partial x} \right) r dr + c.c. = 0$$

terminal condition:

$$\chi_f \int_0^{\infty} \bar{\mathbf{q}}_f^* A_{0f} \mathbf{q}_f r dr + c.c. = 0$$

$$\bar{\chi}_f A_{1f}^T \mathbf{q}_f^* + \gamma_f \mathbf{q}_f + c.c. = 0$$

boundary condition:

$$[\bar{\chi}_f r A_0^T \mathbf{q}^*]_{r=0} + c.c. = 0$$

$$[\bar{\chi}_f r A_0^T \mathbf{q}^*]_{r=\infty} + c.c. = 0$$